



Heatwave intensity on the Iberian Peninsula: Future climate projections



Nieves Lorenzo^{a,*}, Alejandro Díaz-Poso^b, Dominic Royé^{b,*}

^a Environmental Physics Laboratory (EphysLab), CIM-UVIGO, Universidade de Vigo, Edificio Campus da Aula, Ourense 32004, Spain

^b Department of Geography, University of Santiago de Compostela, Santiago de Compostela Spain. Praza da Universidade 1, 15782 Santiago de Compostela, Spain

ARTICLE INFO

Keywords:

Heatwave
Intensity
Iberian Peninsula
Climate change
Spatial extent

ABSTRACT

Heatwaves are the most relevant extreme climatic events, particularly in the context of global warming and the related increasing impacts on society and the natural environment. This work presents an analysis of climate change scenarios with simulations from the EURO-CORDEX project using the excess heat factor over the Iberian Peninsula. We focus on climate change projections of the heatwave intensity and spatial distribution, which are evaluated for the near future (2021–2050) relative to a reference past climate (1971–2000). Heatwave projections show a general significant increase in intensity, frequency, duration and spatial extent for the whole region. The average change in heatwave intensity is 104% for the whole Iberian Peninsula for the near future 2021–2050. The largest changes occur in the eastern-central region, rising to 150% for the Mediterranean coast and the Pyrenees. The greater spatial extent of heatwaves strongly suggests increased human exposure, increased energy demand, and implications for fire risk. This spatial trend is predicted to continue in the near future with increases in the maximum spatial heatwave extent ranging from 6% to 8% per decade.

1. Introduction

The rising global surface temperatures due to global warming are accompanied by extreme events that have increasing impacts on society and the natural environment. In this context, the most relevant extreme climatic events are heatwaves, unusual periods of excessive heat, due to their significant contribution to heat-related morbidity and mortality, social vulnerability, and economic losses in agriculture (Wolf and McGregor, 2013; Zander et al., 2015; Guo et al., 2017; Liss et al., 2017; Royé et al., 2020). Furthermore, the increase in surface temperature affects the frequency and intensity of extreme weather events (Perkins et al., 2012; IPCC Intergovernmental Panel on Climate Change, 2014; Schleussner et al., 2017). In recent years extreme heatwaves have occurred over Europe in 2003, 2010, 2015, and 2018 (Kuglitsch et al., 2010; Russo et al., 2015; Molina et al., 2020). Climatic projections predict more intense, prolonged and frequent extreme heat events in Europe in the 21st century, with a higher impact on the Iberian Peninsula and Mediterranean regions (Fischer and Schär, 2008; IPCC Intergovernmental Panel on Climate Change, 2014; Gasparrini et al., 2017; King and Karoly, 2017; Guerreiro et al., 2018; Dosio et al., 2018; Vicedo-Cabrera et al., 2018). Heatwave events can be characterised by four dimensions: frequency, duration, intensity, and spatial extent (Raei et al., 2018). However, the intensity (also called severity or magnitude)

and the spatial extent of heatwaves have been less studied, particularly on the Iberian Peninsula (Lhotka and Kysely, 2015; Molina et al., 2020; Sánchez-Benítez et al., 2020). However, there is no standard definition or universal statistical approach of defining a heatwave due to the complex interactions between the atmospheric event and the human impacts; and the range of criteria makes it difficult to determine universal measures of any climate (Montero et al., 2013; Perkins and Alexander, 2013). There is also no clear definition for the initiation and of the intensity of a heatwave. For instance, some studies use relative thresholds (95th percentile of daily mean temperature and similar) to define heatwave intensity by comparing the relative health risks associated with different temperature thresholds (Son et al., 2014; Gao et al., 2015; Xu et al., 2016). In other climate studies, it is defined as the sum of the magnitudes (sum of daily maximum temperatures) of different subheat waves in three consecutive days composing a heatwave (Heat Wave Magnitude Index daily) (Russo et al., 2015). In other work with a human health-related perspective, the daily intensity is considered the difference between the daily mean temperature and the 95% percentile of the average temperature combined with an acclimatisation component (Nairn and Fawcett, 2015). The Excess Heat Factor (EHF) developed by Langlois et al. (2013) and Nairn and Fawcett (2015) directly incorporate the aspect of intensity and the acclimatisation process of the human body, which is not included in many of the other heatwave indices (Xu

* Corresponding author.

E-mail addresses: nlorenzo@uvigo.es (N. Lorenzo), dominic.roye@usc.es (D. Royé).

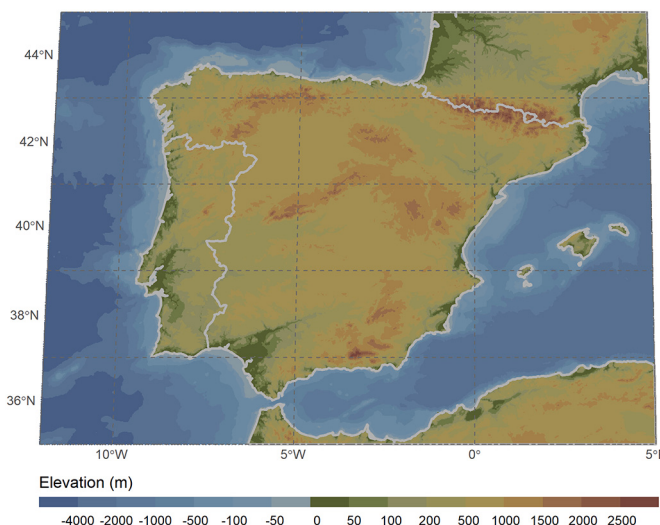


Fig. 1. Study area showing the boundaries of the Iberian Peninsula and terrain elevation.

et al., 2016). The EHF is a two-component index. The first component is the comparison of the three-day average daily mean temperature with the 95th percentile. The second component is a measure of the temperatures reached during the three-day period compared with the recent past (the previous 30 days). Knowledge and comprehension of the effect that different elements defining a heatwave have on human health are essential to the health system (Guo et al., 2011; Royé et al., 2020). Climate change adaptation plans should consider the different dimensions of heatwaves, not only extreme heatwave events or national scales. Moreover, they should consider the demands of health services at the local and regional levels. Previous studies suggest that the EHF can better predict health risk events compared with other heatwave indices (Scalley et al., 2015; Guo et al., 2017; Williams et al., 2018; Royé et al., 2020). Thus, given the importance of adapting health systems to climate change in the future (Nairn et al., 2018), we suggest that future scenarios of heatwaves for the Iberian Peninsula, based on the EHF, should be estimated, emphasising possible changes in intensity and spatial extent. In this study, we used temperature projections for the period 2021–2050 under two future warming scenarios (Representative Concentration Pathway RCP4.5 and RCP8.5) from the EURO-CORDEX project.

2. Data and methods

2.1. Model simulations

To generate climate change projections, daily temperature data from five simulations and two future scenarios of the CORDEX project (<http://www.euro-cordex.net/>) were obtained. This project offers model simulations over Europe at a high spatial resolution of approximately 12 km (0.11°), which are driven by global climate simulations from the Coupled Model Intercomparison Project Phase 5 (CMIP5) long experiments up to the year 2100 (Moss et al., 2010; Taylor et al., 2012; Jacob et al., 2014). The high spatial resolution of these data allows us to incorporate regional physiographic characteristics (topography, vegetation, coastline, etc.) relevant for specific impact and vulnerability studies and assessing the need for adaptation to climate change at a more local scale.

Maxima and minima temperature simulations over the Iberian Peninsula (Fig. 1) were obtained from one Regional Climate Model (RCM), driven by five different global climate models (GCMs) over the period 1971–2050. The chosen regional model RCA4 of the Swedish Meteorological and Hydrological Institute generally performs well when

Table I
Models included in the analysis.

Project	GCMs	RCM
EURO-CORDEX	CNRM-CM5 EC-EARTH ICHEC IPSL-CM5A-MR HadGEM2-ES-MOHC MPI-ESM-LR	RCA4

simulating the recent past climate taking boundary conditions from the Global Climate Models (GCMs). RCA4 is easily transferable and applicable for any domain worldwide and is efficient and user-friendly to operate. For more details on this climate model, the reader is referred to the page (<https://na-cordex.org/rcm-characteristics.html>). A brief description of global climate models can be found in Jacob et al. (2014) or Taylor et al. (2012).

The temperature values of the models were evaluated for the reference period (1971–2000), and the climate change impact on heatwaves was characterised considering the differences between a near-future period (2021–2050) and the historical reference period (1971–2000). Future temperature data were obtained from climate projections for two scenarios, RCP4.5 and RCP8.5. These two scenarios allow the analysis of future projections under an intermediate scenario of greenhouse gas emissions and concentrations and a scenario with a very high level of emissions (RCP8.5) (Moss et al., 2010). Table I lists the simulations considered from the CORDEX project.

2.2. Excess Heat Factor

The EHF is a recent measure of heatwave intensity developed by Langlois et al. (2013). This index is based on a three-day average daily mean temperature. The three-day period is motivated by studies of human responses to the onset of extremely hot weather. The main reason for measuring heatwave intensity is to identify the heatwaves that could potentially inflict severe consequences on the population (Langlois et al., 2013; Nairn and Fawcett, 2015; Scalley et al., 2015). The EHF is a factorisation of two excess daily heat indices.

The first is the comparison of the three-day average daily mean temperature with the temperature threshold in that specific location for the whole study period (1971–2000, 2021–2050). Suppose the average of the daily mean temperature during the three-day period is higher than the 95th climatological percentile for the daily mean temperature. In that case, this three-day period falls under heatwave conditions. This component is called the significance index (EHIsig_i). If it is positive, the period is deemed to be unusually warm compared with the local annual climate.

$$EHIsig_i = \frac{(T_i + T_{i+1} + T_{i+2})}{3} - T_{95}$$

where: i is each day of the whole study period, T the daily mean temperature and T_{95} the 95th percentile of the daily mean temperature for each time period.

The second component of the EHF is a measure of the temperatures reached during the three-day period compared with the recent past (the previous 30 days). This second component is the acclimatisation index (EHIconcl_i) (Nairn and Fawcett, 2015).

$$EHIconcl_i = \frac{(T_i + T_{i+1} + T_{i+2})}{3} - \frac{(T_{i-1} + \dots + T_{i-30})}{30}$$

The calculation of the heatwave intensity (EHF) is designed to treat the acclimatisation index (EHIconcl_i) as an amplifying factor for the significance index (EHIsig_i) that does not reduce the significance of the climate threshold excess heat. EHIsig_i is only amplified when EHIconcl_i is greater than 1 and only values of EHFi > 0 can be considered heatwave days.

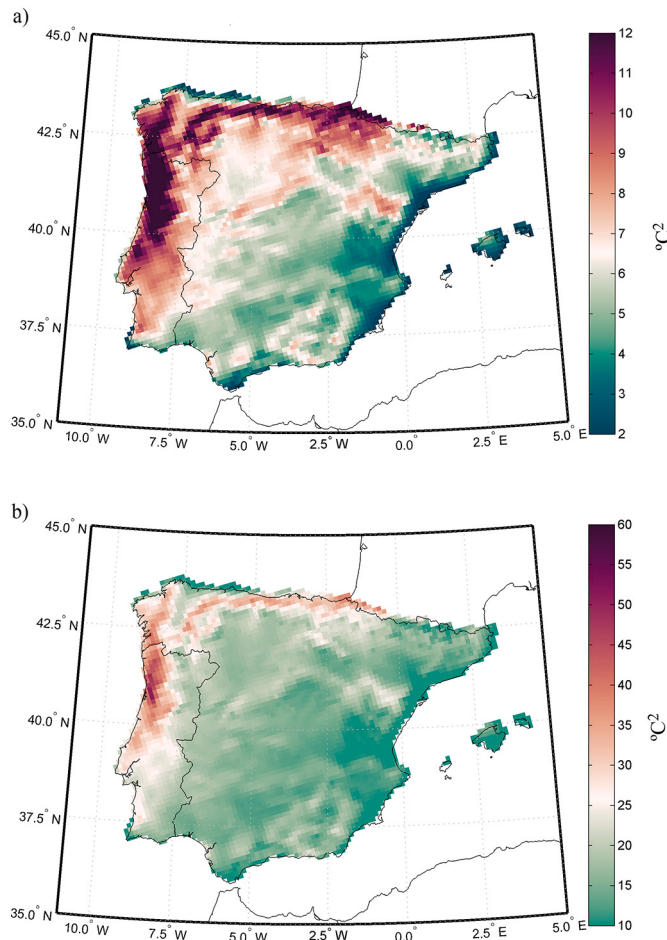


Fig. 2. a) Annual average positive EHF (spatial average: $6.5 \text{ }^{\circ}\text{C}^2$) and b) annual EHF_{max} for the period 1971–2000 ($\text{ }^{\circ}\text{C}^2$) (spatial average: $25.8 \text{ }^{\circ}\text{C}^2$).

$$\text{EHF}_i = \text{EHIsig}_i \cdot \max(1, \text{EHlacc}_i)$$

The severity of the heatwave was also considered. This severity threshold is determined by the 85th percentile (P85) of all positive EHF values in the study period; with this percentile, it is possible to separate normal from extreme events (Langlois et al., 2013). The present work, following the study of Nairn and Fawcett (2015), considers that a heatwave will be extreme if EHF is three times EHF_{P85}. According to this, the three degrees of severity are: low severity ($\text{EHF}/\text{EHF}_{\text{P85}} \leq 1$), severe ($1 < \text{EHF}/\text{EHF}_{\text{P85}} < 3$), and extreme ($\text{EHF}/\text{EHF}_{\text{P85}} \geq 3$).

2.3. Analysis

Future projections were evaluated using the multimodel ensemble mean of the five simulations. The future scenario-run data—covering the period 2021 to 2050—were used in conjunction with the reference-run data (1971–2000) to obtain the climate change signal simulated by the RCMs by applying the commonly used “delta method”. For each of the values analysed, the mean value of the 1971–2000 control integration was subtracted from the mean value of the 2021–2050 scenario integration (Lenderink et al., 2007). With this delta the percentage of change in the values calculated under the two scenarios RCP4.5 and RCP8.5 is analysed. To test for significant changes ($\alpha = 0.05$), a two-sided Wilcoxon rank-sum test was applied. The two-sided Wilcoxon rank-sum test is a nonparametric test for two independent samples (Wilcoxon, 1945). It can be used to evaluate whether the distributions of two independent samples are systematically different from one another.

To observe future changes in the different heatwave dimensions

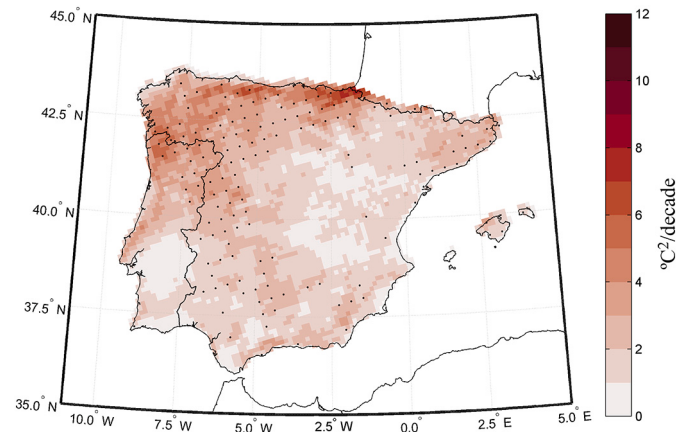


Fig. 3. Trend in the annual maximum of EHF for the period 1971–2000. Values are expressed as $(^{\circ}\text{C}^2)/\text{decade}$. Black dots: significant trends at $\alpha = 0.05$.

based on the EHF, we estimated the annual average and maximum EHF value (intensity), the average heatwave days (EHF > 0), the heatwave event duration (consecutive days with EHF > 0) and the average and maximum relative spatial extent (EHF > 0 relative proportion of all points) for the study area during the historical (1971–2000) and near future (2021–2050) period. The trend analysis is based on the nonparametric Mann-Kendall test (Mann, 1945; Kendall, 1975), with a

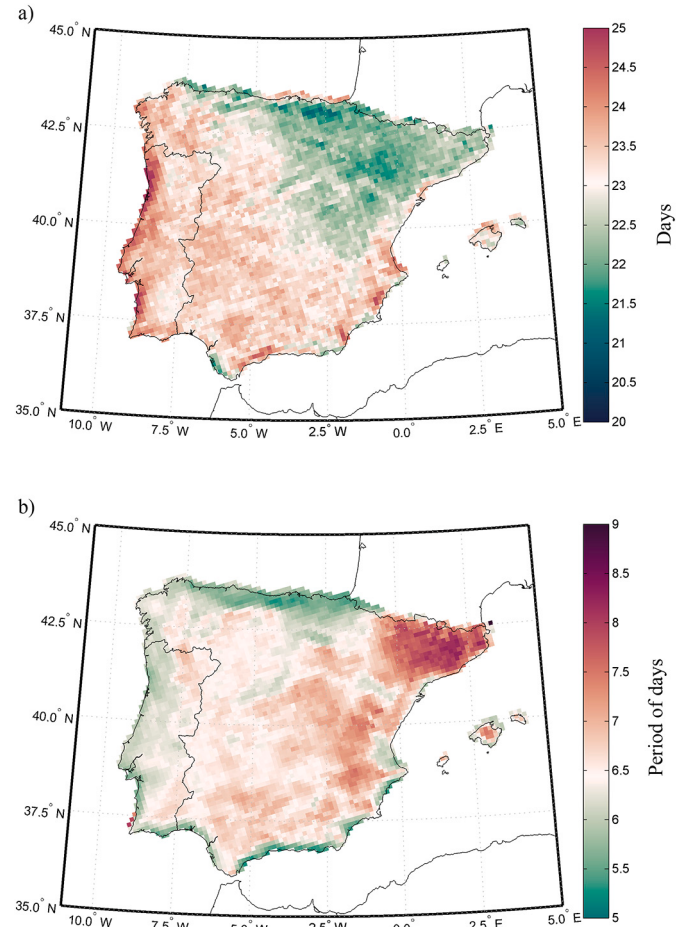


Fig. 4. a) The annual average number of heatwave days (the spatial average is 23 days) and b) the annual duration of the periods considered to be a heatwave (the spatial average is 6 days) for 2021–2050.



Fig. 5. Trend in the number of heatwave days for the period 1971–2000. Values are expressed in days/decade. Black dots: significant trends at $\alpha = 0.05$.

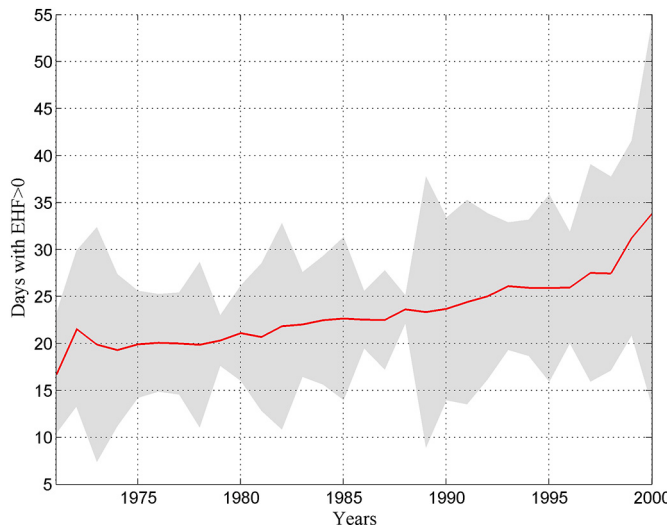


Fig. 6. Time series of annual heatwave days on the Iberian Peninsula from 1971 to 2000. The green shaded area is the confidence interval.

confidence level of 95%. This test is nonparametric and is widely used in the analysis of environmental data. One of its benefits is that the data do not need to conform to any particular distribution.

The main results are presented with respect to the whole Iberian Peninsula to emphasise the spatial differences. The reason for this is that, while heatwaves will increase for the whole study area due to the expected global warming, it is very likely to observe regional differences.

3. Results

3.1. Excess Heat Factor trends during 1971–2000

The temporal trends of the EHF observed during the historical period 1971–2000 demonstrate high regional variability. Fig. 2 shows the average positive EHF (a) and the EHF_{max} (b) for 1971–2000. These results were calculated based on the ensemble of the five CORDEX models as described in the data section. The average of the positive EHF over the whole Iberian Peninsula is 6.5°C^2 .

The spatial pattern does not depend on latitude for the average EHF, as seen by Nairn and Fawcett (2015) in Australia. However, in general, a continental and, particularly, an altitudinal effect can be observed. The

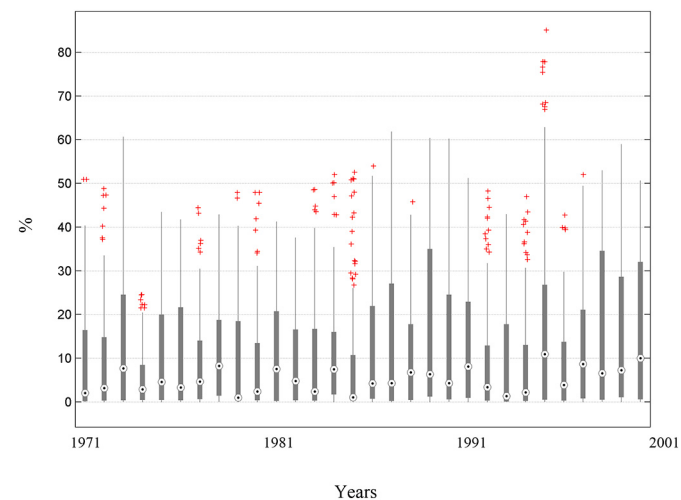


Fig. 7. Distribution of the heatwave extent per year on the Iberian Peninsula (1971–2000).

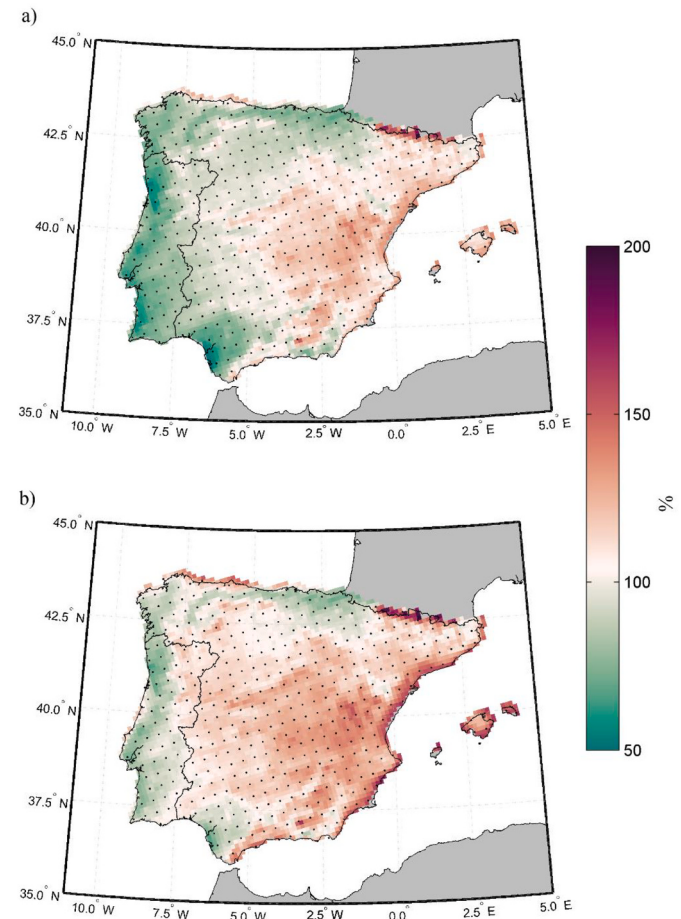


Fig. 8. Percentage of change in the number of heatwave days for the period 2021–2050 with respect to the period 1971–2000 for both scenarios, a) RCP4.5 and b) RCP8.5. Black dots: significant change at $\alpha = 0.05$.

highest values are located in the west of the Iberian Peninsula, in the eastern Cantabrian and the Cantabrian mountain range, and the lowest values are found in the Mediterranean coastal areas. The pattern of the EHF_{max} (Fig. 2b) is similar to that of the average EHF with its spatial average of 25.8°C^2 , and higher values can be found in the same areas as

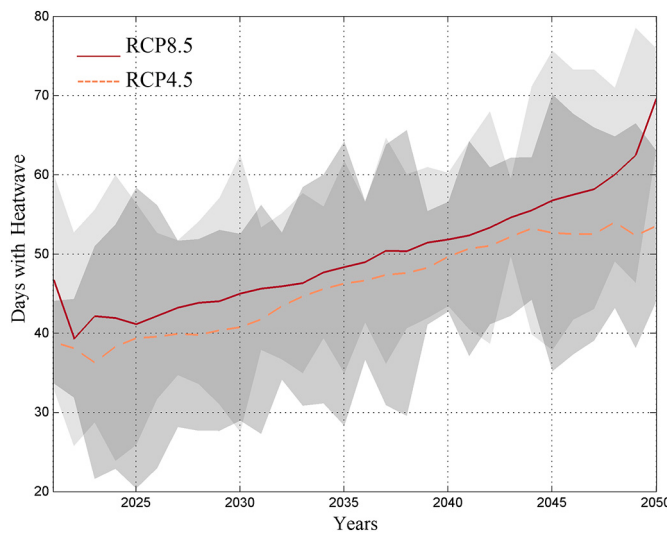


Fig. 9. Time series of heatwave days on the Iberian Peninsula from 2021 to 2050. The orange dashed line is the RCP4.5 scenario and the solid red line the RCP8.5 scenario.

those of the mean EHF. Although the trend of EHF oscillates between 0 and 2°C^2 per decade, we observe an increase of between 2 and 6°C^2 per decade for the EHF_{max} trend (Fig. 3) with the highest EHF_{max} values mainly localised in the north and west of the Iberian Peninsula. The spatial average number of heatwave days for the whole peninsula is approximately 23 days, oscillating between 20 and 25 days due to the regional variability (Fig. 4a).

The duration of the heatwave was 6 days on average (Fig. 4b). In the central-eastern Iberian Peninsula, the duration of heatwaves was longer, especially in Catalonia and the Balearic Islands, where the heatwave could last more than 8 days. Although the intensity is greater in the central-western part of the Iberian Peninsula (Fig. 2), the heatwaves were less persistent in this area because it is more exposed to the arrival of mild air masses from the Atlantic Ocean. The estimated trends in the number of heatwave days during 1971–2000 show an increase of 4 days/decade across almost the whole territory and particularly in the central northern Iberian Peninsula (Fig. 5).

This positive trend is clear in Fig. 6 that presents the annual time series of the heatwave days on the Iberian Peninsula from 1971 to 2000, with an average spatial trend over the peninsula of 3.8 days/decade.

In addition to heatwave intensity and duration, another factor to consider is the average and maximum annual spatial distribution of heatwave days (Fig. 7). Considerable intra- and interannual variability can be observed in the extent of the heatwaves. From 1971 to 2000 there was an increasing trend of 1.7% per decade in the average annual extent and an increase of 4.3% per decade in the maximum extent.

3.2. Projected changes in the Excess Heat Factor for the near future period 2021–2050

The percentage of change projected by the simulations for the average annual number of heatwave days is shown in Fig. 8. In both RCPs, the spatial average change was 104% for the whole peninsula; the more remarkable changes occurred in the central-eastern region, rising to a value of 150% along the Mediterranean coast and the Pyrenees.

In the RCP4.5 scenario, the greatest changes were confined to the central-eastern Iberian Peninsula, while in the RCP8.5 scenario, high values affected practically the whole territory, excluding a constricted band along the Atlantic coast and part of the Bay of Biscay. These changes resulted in an annual mean of between 30 and 65 heatwave days per year for 2021–2050. Thus, the ensemble mean model predicted

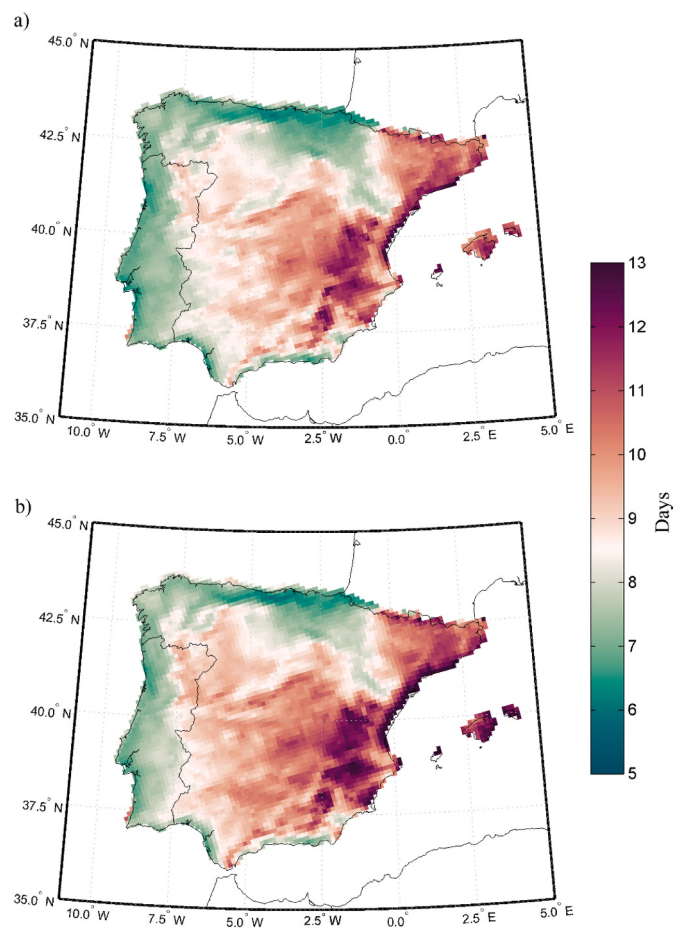


Fig. 10. Change of heatwave duration (spatial average of 8 days).

a predominant increase in the number of heatwave days per year over the Iberian Peninsula with an overall positive trend of 6.4 days/decade in the RCP4.5 scenario and 7.6 days/decade in the RCP8.5 scenario. The projected trends double those observed in the period 1971–2000 (Fig. 9). The differences between the two scenarios will increase from the second half of the 21st century onwards when the scenarios begin to display more different behaviour with a greater temperature increase in the RCP8.5 scenario (IPCC Intergovernmental Panel on Climate Change, 2014). (See Fig. 10.)

The duration of heatwaves showed an increase with values greater than 15 days in the Mediterranean region and a minimum of 6 days in the northern and western regions (Fig. 10). Moreover, in the RCP8.5 scenario, prolonged heatwaves (> 10 days) extended over practically the whole peninsula, except for the Atlantic coast, where the duration oscillated between 6 and 7 days. A spatial trend analysis of the annual number of heatwave days shows that the highest values are located in the Pyrenees, inland and south of the Iberian Peninsula (Fig. 11).

Heatwaves are expected to be more intense in both future scenarios; hence in the analysis of EHF_{Max} we can see how the change ranged between 60% and 80% in the RCP4.5 scenario and was almost 100% across most of the peninsula in the RCP8.5 scenario (Fig. 12). The average change was around 65% for most of the Iberian Peninsula in both RCPs. These observed changes led to an EHF_{Max} greater than 25°C^2 for most of the Iberian Peninsula (Fig. A.1).

The spatial distribution of heatwave days showed a positive increasing trend at the annual scale compared with the 1971–2000 reference period (Fig. 13). The interquartile range (difference between 25th and 75th percentile) increased in both scenarios, indicating that 50% reached a wider spatial extent, with the median also considerably

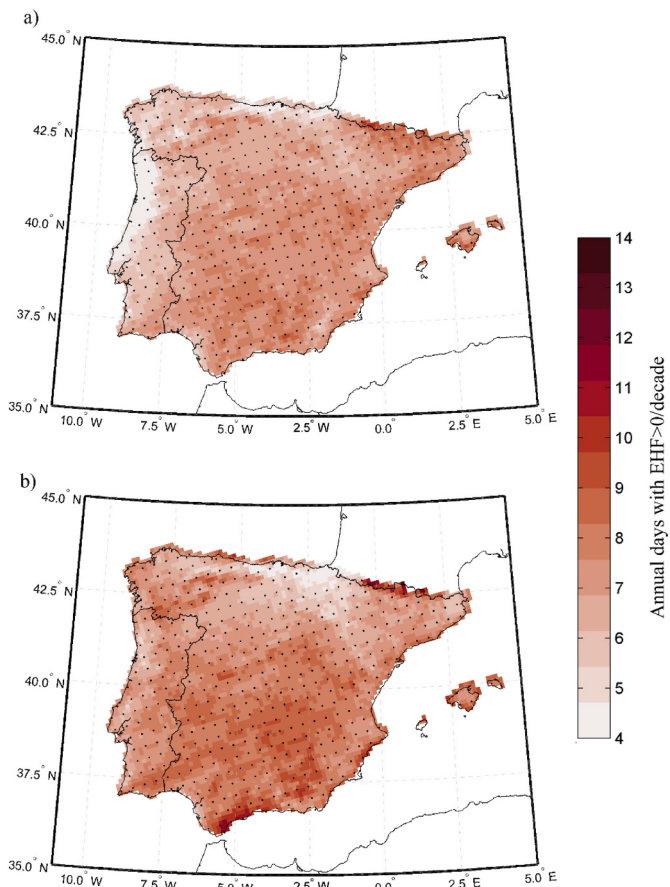


Fig. 11. Trend in the number of heatwave days for the period 2021–2050 in scenarios a) RCP4.5 and b) RCP8.5. Values are expressed in days/decade. Black dots: significant change at $\alpha = 0.05$.

higher. Heatwaves cover an increasing area of the peninsula, and they far exceeded 50% of the extent in a large number of years. Moreover, it is interesting to note that the upper limit exceeded 70% in the Iberian Peninsula in 50% of the years during the RCP4.5 scenario. In 80% of the years in the RCP8.5 scenario, these values were very rare in the reference period 1971–2000. The trend of the average annual extent of heatwaves in the Iberian Peninsula was approximately 3.6% per decade and 2.5% per decade, respectively. Conversely, the increase in the maximum extent reached 7.9% per decade and 5.7% per decade, respectively.

Fig. 14 presents the net change in the number of days of each heatwave severity level. The increase in the average number of days in each severity level for both scenarios was 64, 18 and 9 days, respectively. Extreme events increased mainly in the coastal areas. In contrast, severe and low-intensity events increased more along the Mediterranean coast and in the inland regions. However, low severity events seem to increase from east to west.

The EHF projections are summarised in Fig. 15, where the number of heatwaves, the intensity of EHF_{max} , and the mean and maximum extent are presented for the historical period and future projections. While the median value of heatwaves during 1971–2000 is around 23 days, the median heatwave number increased to 44 days in RCP4.5, and 50 days in RCP8.5. All heatwave dimensions will increase for the RCP scenarios. The median value of EHF_{max} will double in RCP4.5, and for RCP8.5 an increase from 11 to 24 $^{\circ}\text{C}^2$ is expected. The spatial extent of heatwaves will almost double in RCP8.5 for the period 2021–2050.

Discussion and conclusions.

This study was motivated by the lack of analysis of the heatwave

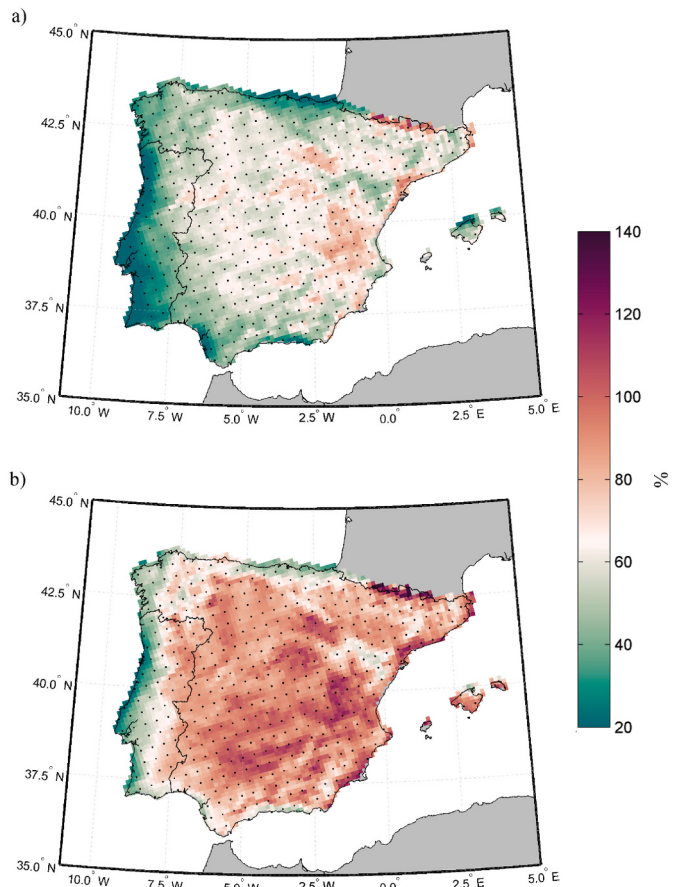


Fig. 12. Changes in projected EHF_{Max} index (%) for the period 2021–2050 compared with 1971–2000 for RCP4.5 (a) and RCP8.5 (b). Black dots: significant change at $\alpha = 0.05$. (average value is 65%).

spatial extent and intensity for the Iberian Peninsula. We analysed heatwave dimension intensity, frequency, duration and extent on the Iberian Peninsula for historical (1971–2000) and near-future (2021–2050) periods in projected scenarios RCP4.5 and RCP8.5 using the EHF, which led to important new insight. Furthermore, we used models with a high spatial resolution, which allowed us to discern the regions that may be more or less susceptible to heatwaves due to their geographic characteristics.

In the analysed 1971–2000 period, the intensity dimension described by the EHF was higher in the western peninsular and mountainous areas. This observation is likely related to the presence of a high-altitude dorsal from North Africa that causes a warm air injection into high atmospheric layers and occurs in the vast majority of heatwaves affecting the Iberian Peninsula (Tullot, 2000; Gil Olcina and Gómez-Mendoza, 2001; Rodríguez-Puebla et al., 2010; Merino et al., 2018). The pattern of the average EHF and the maximum EHF can be explained in the same way. The observed positive trends in these parameters are higher in the maximum EHF value, which means that heatwaves will have a higher heat excess; hence heatwave days will become more intense.

It should be noted that the areas showing a higher intensity do not coincide with areas where heatwave events have a longer duration. For both 1971–2000 and 2021–2050, heatwaves in the western peninsular and mountainous regions are characterised by a higher EHF but a shorter duration than those in the southeast peninsular area and, in general, on the Mediterranean coast. The main reason for this spatial pattern lies in the rapid transport of mild air masses from the Atlantic Ocean into the western Iberian Peninsula.

The heatwave day frequency also increases, and for the near future

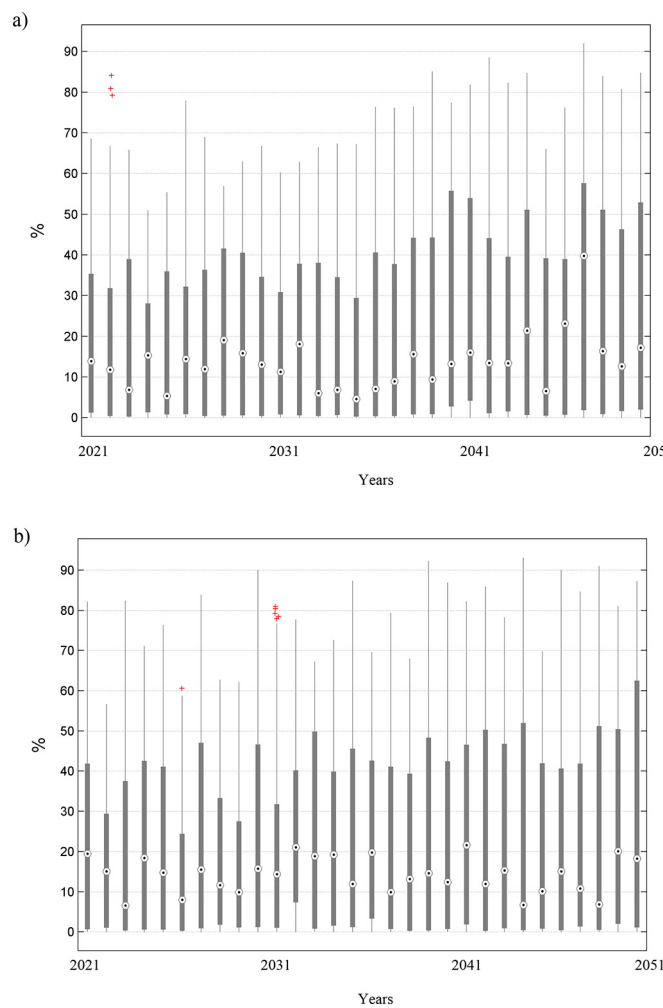


Fig. 13. Distribution of heatwave extent per year on the Iberian Peninsula (2021–2050), a) RCP4.5 and b) RCP8.5.

2021–2050 there was an increase of 150% in the number of heatwave days compared with 1971–2000 for the Mediterranean coast. The EHF not only shows an increase in the intensity of heatwave days but also indicates an increase in the frequency of these events following observations using other heatwave indices in previous work (Rodríguez-Puebla et al., 2010; Ramos et al., 2011; Andrade et al., 2012; Russo et al., 2014; Pereira et al., 2017; Viceto et al., 2019).

In addition, our results of the EHF projections show substantial increases in the spatial extent and duration. The increased spatial extent of heatwaves strongly suggests increased human exposure, increased energy demand, as well as implications for fire risk. In the period 1971–2000 the average duration of heatwave events was 6 days, whereas for 2021–2050 a 10-day duration is predicted as the new normal for an important area of the Iberian Peninsula. The average extent of heatwaves for the period 1971–2000 has increased by 1.71% per decade, while the increase in the maximum extent is even greater at 4.3% per decade. This trend is expected to continue in the near future, with increases ranging from 6% to 8% per decade for the maximum extent value. The results point towards a significant increase in the intensity, frequency, duration and extent of heatwaves over the Iberian Peninsula by the 21st century in RCP4.5 and RCP8.5. These results are in agreement with studies on heatwaves carried out with other indices for Europe and the contiguous US (Fischer and Schär, 2010; Burkett et al., 2014; Schoetter et al., 2015; Lhotka and Kyselý, 2015; Lyon et al., 2019; Molina et al., 2020).

The EHF index is better at detecting heatwave conditions than other

indices making it a useful tool to contribute to decision-making that minimises the negative impacts of heatwaves on public health or in other susceptible sectors such as agriculture, forestry or energy. Previous studies showed that the EHF could be used to assess the health effects of heatwaves at the population level (Jian et al., 2015; Royé et al., 2020). Royé et al. (2020) showed that city-specific exposure-response curves in Spain have a non-linear J-shaped relationship between mortality and the EHF. It is essential to acknowledge that heatwave periods do not show the same degree of intensity every day. In the context of our results for future projections, the intensity will increase substantially with significant negative impacts on human health.

Further research should focus on heatwaves and their relationship with large-scale atmospheric circulation, land-use/atmosphere interactions, such as the interaction between urban heat islands, and heatwaves in the current and future climates. Furthermore, extending this study to the period 2051–2100 would allow the observation of greater differences between the RCP4.5 and RCP8.5 scenarios until the end of the century. On the other hand, the issue of uncertainty is at the heart of the climate change prediction problem. Due to its complexity, both conceptual and applied to specific impact issues, it will remain a central issue within the climate change debate (Giorgi, 2010). Therefore, in this study, we considered the uncertainties as a multimodel ensemble mean of 5 model projections. Ensembles of model simulations represent a fundamental resource for studying the range of plausible climate responses to a given forcing (Meehl et al., 2007; Randall et al., 2007). In general, climate models simulate observed changes in extreme

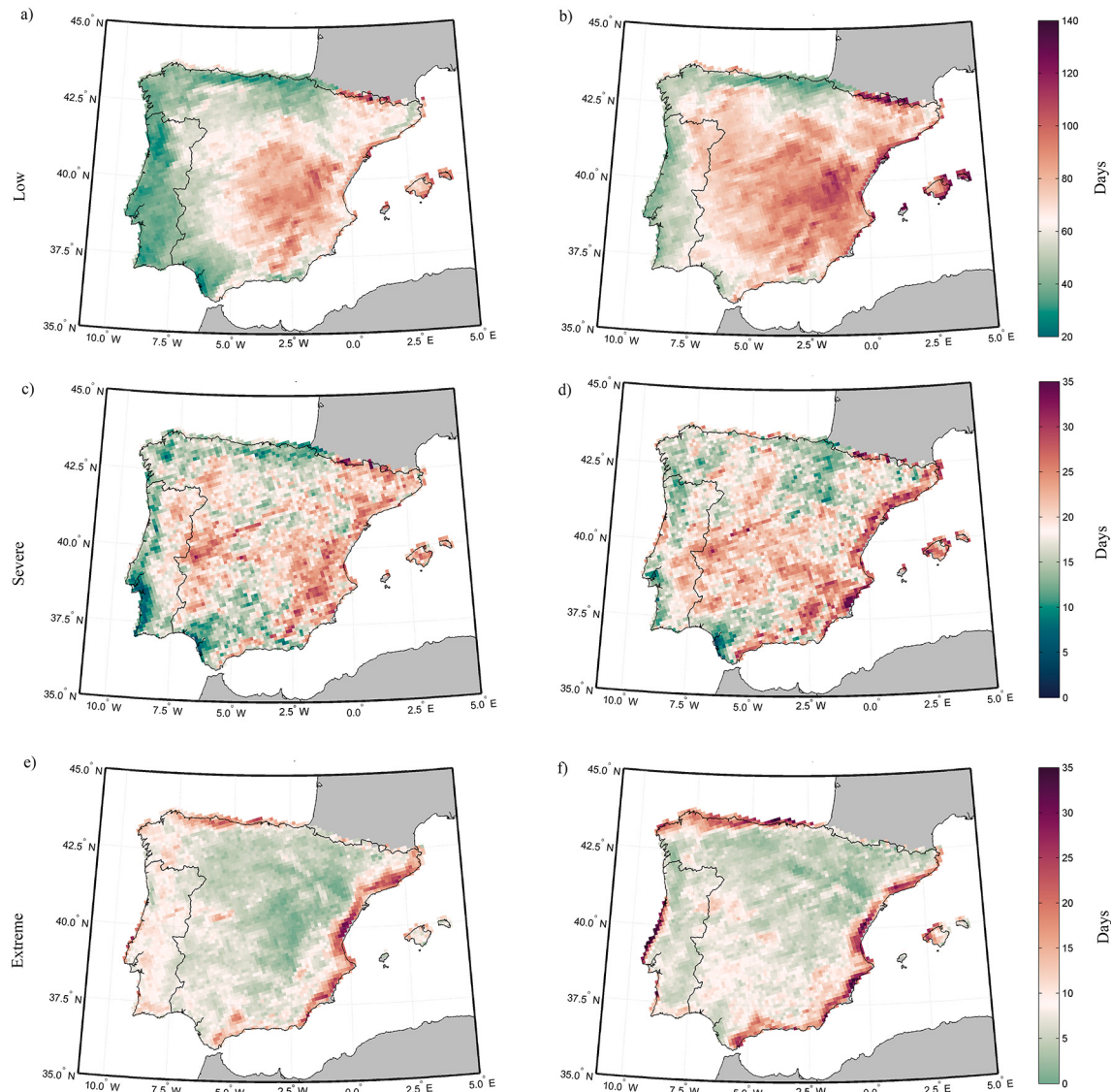


Fig. 14. Change in the severity index based on EHF for a) RCP4.5 and b) RCP8.5.

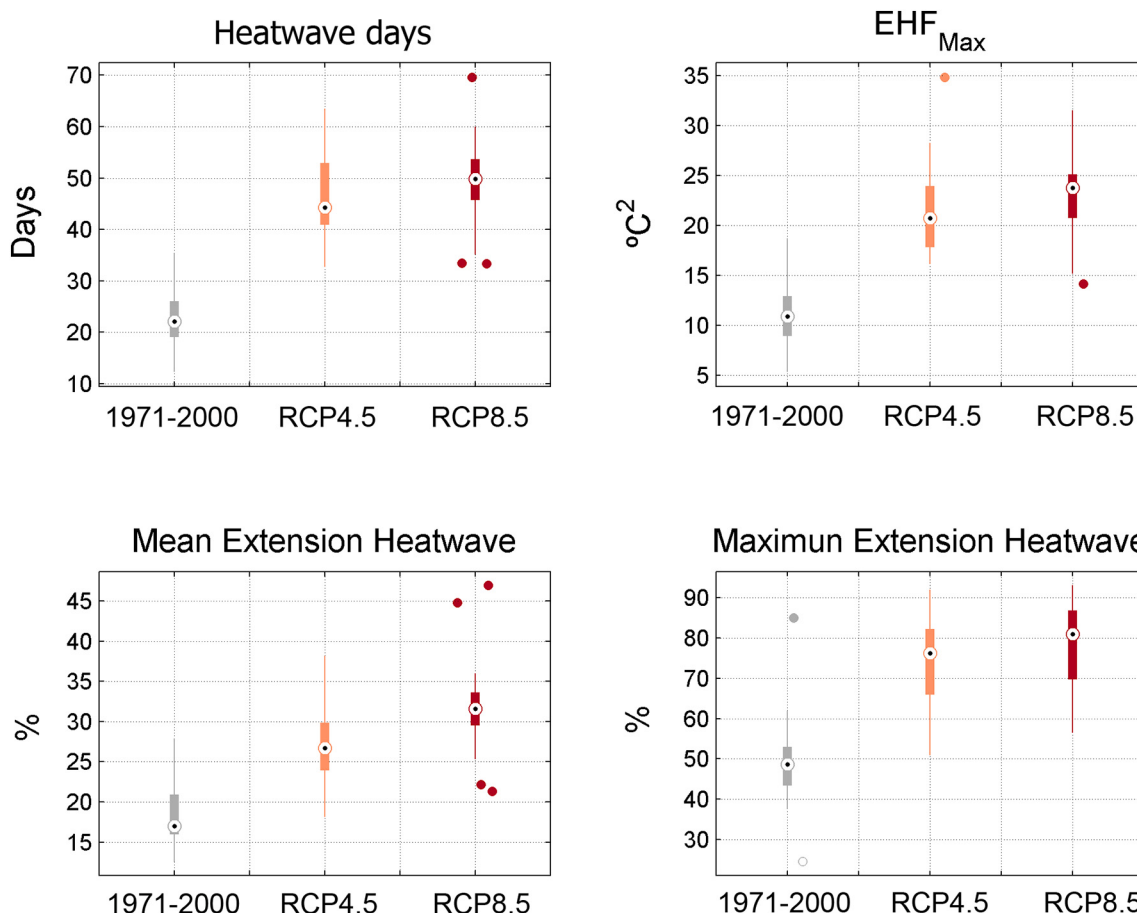


Fig. 15. The EHF projection summary as box-whisker plots for the Iberian Peninsula. The point indicates the median, the boxes the interquartile range and the whisker the observed range.

temperatures relatively well, and projections of changes in temperature extremes tend to be consistent across climate models (in terms of sign) (Randall et al., 2007). However, for the next study, a full characterisation of uncertainty will require large ensembles of model projections and maybe do an analysing of the spatial uncertainties like in previous works (Wu et al., 2021).

Supplementary data to this article can be found online at <https://doi.org/10.1016/j.atmosres.2021.105655>.

Declaration of Competing Interest

The authors declare that they have no known competing financial interests or personal relationships that could have appeared to influence the work reported in this paper.

Acknowledgments

The authors thank the WCRP's Working Group on Regional Climate, and the Working Group on Coupled Modelling, former coordinating body of CORDEX and responsible panel for CMIP5. We also thank the climate modelling groups for producing and making available their models' outputs that can be downloaded at <http://www.cordex.org/>.

This work was partially financed by Xunta de Galicia (Spain) under project ED431C 2017/64 "Programa de Consolidación e Estructuración de Unidades de Investigación Competitivas".

References

- Andrade, C., Leite, S.M., y Santos, J.A., 2012. Temperature extremes in Europe: overview of their driving atmospheric patterns. *Nat. Hazards Earth Syst. Sci.* 12, 1671–1691. <https://doi.org/10.5194/nhess-12-1671-2012>.
- Burkett, V.R., Suarez, A.G., Bindu, M., Conde, C., Mukerji, R., Prather, M.J., Clair, A.L.S., Yohe, G.W., 2014. Point of departure. In: Field, C.B., Barros, V.R., Dokken, D.J., Mach, K.J., Mastrandrea, M.D., Bilir, T.E., White, L.L. (Eds.), *Climate Change 2014: Impacts, Adaptation, and Vulnerability. Part A: Global and Sectoral Aspects*. Contribution of Working Group II to the Fifth Assessment Report of the Intergovernmental Panel of Climate Change. Cambridge University Press, Cambridge, pp. 169–194.
- Dosio, A., Mentaschi, L., Fischer, E.M., Wyser, K., 2018. Extreme heat waves under 1.5°C and 2°C global warming. *Environ. Res. Lett.* 13, 054006 <https://doi.org/10.1088/1748-9326/aab827>.
- Fischer, E.M., Schär, C., 2008. Future changes in daily summer temperature variability: driving processes and role for temperature extremes. *Clim. Dyn.* 33, 917–935. <https://doi.org/10.1007/s00382-008-0473-8>.
- Fischer, E.M., Schär, C., 2010. Consistent geographical patterns of changes in high-impact European heatwaves. *Nat. Geosci.* 3 (6), 398–403. <https://doi.org/10.1038/ngeo866>.
- Gao, J., Sun, Y., Liu, Q., Zhou, M., Lu, Y., Li, L., 2015. Impact of extreme high temperature on mortality and regional level definition of heat wave: a multi-city study in China. *Sci. Total Environ.* 505, 535–544. <https://doi.org/10.1016/j.scitotenv.2014.10.028>.
- Gasparrini, A., Guo, Y., Sera, F., Vicedo-Cabrera, A.M., Huber, V., Tong, S., Armstrong, B., 2017. Projections of temperature-related excess mortality under climate change scenarios. *Lancet Planet. Health.* 1, e360–e367. [https://doi.org/10.1016/S2542-5196\(17\)30156-0](https://doi.org/10.1016/S2542-5196(17)30156-0).
- Gil Olcina, A., Gómez-Mendoza, J. (Eds.), 2001. *Geografía de España*. Barcelona, Geografía, Editorial Ariel.
- Giorgi, F., 2010. 2010 Uncertainties in climate change projections, from the global to the regional scale. *EPJ Web Conf.* 9, 115–129. <https://doi.org/10.1051/epjconf/201009009>.
- Guerreiro, S.B., Dawson, R.J., Kilsby, C., Lewis, E., Ford, A., 2018. Future heat waves, droughts and floods in 571 European cities. *Environ. Res. Lett.* 13 (3), 034009. <https://doi.org/10.1088/1748-9326/aaaad3>.

- Guo, Y., Barnett, A., Pan, X., Yu, W., Tong, S., 2011. The impact of temperature on mortality in Tianjin, China: a case-crossover design with a distributed lag non-linear model. *Environ. Health Perspect.* 119, 1719–1725. 10.1289%2Fehp.1103598.
- Guo, Y., Gasparini, A., Armstrong, B.G., Tawatsupa, B., Tobias, A., Lavigne, E., Coelho, M.S.Z.S., Pan, X., Kim, H., Hashizume, M., Honda, Y., Guo, Y.L., Wu, C.F., Zanobetti, A., Schwartz, J.D., Bell, M.L., Scorticichini, M., Michelozzi, P., Punnasiri, K., Li, S., Tian, L., Garcia, S.D.O., Seposo, X., Overcenco, A., Zeka, A., Goodman, P., Dang, T.N., Dung, D.V., Mayvaneh, F., Saldiva, P.H.N., Williams, G., Tong, S., 2017. Heat wave and mortality: a multicountry, multicommunity study. *Environ. Health Perspect.* 125 <https://doi.org/10.1289/EHP1026>, 0870061–11.
- IPCC Intergovernmental Panel on Climate Change, 2014. *IPCC Intergovernmental Panel on Climate Change. In: Climate Change 2014—Impacts, Adaptation and Vulnerability: Regional Aspects*. Cambridge University Press.
- Jacob, D., Petersen, J., Eggert, B., et al., 2014. EURO-CORDEX: new high-resolution climate change projections for European impact research. *Reg. Environ. Chang.* 14, 563–578. <https://doi.org/10.1007/s10113-013-0499-2>.
- Jian, L., Scalley, B., Xiao, A., Nairn, J., Spicer, T., Somerford, P., Ostendorf, B., Weeramanthri, T., 2015. Is excess heat factor a good indicator for assessing heatwave related health outcomes in Western Australia? *Int. J. Epidemiol.* 44 (1), i65. <https://doi.org/10.1093/ije/dyv097.241>.
- Kendall, M.G., 1975. *Rank Correlation Methods*. Charles Griffin, London, p. 120.
- King, A.D., Karoly, D.J., 2017. Climate extremes in Europe at 1.5 and 2 degrees of global warming. *Environ. Res. Lett.* 12, 114031 <https://doi.org/10.1088/1748-9326/aa8e2c>.
- Kuglitsch, F.G., Toreti, A., Xoplaki, E., Della-Marta, P.M., Zerefos, C.S., Türkş, M., Luterbacher, J., 2010. Heat wave changes in the eastern Mediterranean since 1960. *Geophys. Res. Lett.* 37, L04802 <https://doi.org/10.1029/2009GL041841>.
- Langlois, N., Herbst, J., Mason, K., Nairn, J., Byard, R., 2013. Using the excess heat factor (EHF) to predict the risk of heat related deaths. *J. Forensic Legal Med.* 20, 408–411. <https://doi.org/10.1016/j.jflm.2012.12.005>.
- Lenderink, G., van Ulden, A., van den Hurk, B., Keller, F., 2007. A study on combining global and regional climate model results for generating climate scenarios of temperature and precipitation for the Netherlands. *Clim. Dyn.* 29, 157–176. <https://doi.org/10.1007/s00382-007-0227-z>.
- Lhotka, O., Kyselý, J., 2015. Characterising joint effects of spatial extent, temperature magnitude and duration of heat waves and cold spells over Central Europe. *Int. J. Climatol.* 35, 1232–1244. <https://doi.org/10.1002/joc.4050>.
- Liss, A., Wu, R., Chui, K., Naumova, E., 2017. Heat-related hospitalisations in older adults: an amplified effect of the first seasonal heatwave. *Sci. Rep.* 7, 39581. <https://doi.org/10.1038/srep39581>.
- Lyon, B., Barnston, A.G., Coffel, E., Horton, R.M., 2019. Projected increase in the spatial extent of contiguous US summer heat waves and associated attributes. *Environ. Res. Lett.* 14 (11), 114029. <https://doi.org/10.1088/1748-9326/ab4b41>.
- Mann, H.B., 1945. Nonparametric tests against trend. *Econometrica*. 13, 245–259.
- Meehl, G.A., Stocker, T.F., Collins, W.D., Friedlingstein, P., Gaye, A.T., Gregory, J.M., Kitoh, A., Knutti, R., Murphy, J.M., Noda, A., Raper, S.C.B., Watterson, I.G., Weaver, A.J., Zhao, Z.C., 2007. Global climate projections. In: Solomon, S., Qin, D., Manning, M., Chen, Z., Marquis, M., Averyt, K.B., Tignor, M., Miller, H.L. (Eds.), *Climate Change 2007: The Physical Science Basis. Contribution of Working Group I to the Fourth Assessment Report of the Intergovernmental Panel on Climate Change*. Cambridge University Press, Cambridge, UK, and New York, NY, pp. 747–845.
- Merino, A., Martín, M.L., Fernández-González, S., Sánchez, J.L., y Valero, F., 2018. Extreme maximum temperature events and their relationships with large-scale modes: potential hazard on the Iberian Peninsula. *Theor. Appl. Climatol.* 133, 531–550. <https://doi.org/10.1007/s00704-017-2203-9>.
- Molina, M.O., Sánchez, E., Gutiérrez, C., 2020. Future heat waves over the Mediterranean from an Euro-CORDEX regional climate model ensemble. *Sci. Rep.* 10, 8801. <https://doi.org/10.1038/s41598-020-65663-0>.
- Montero, J., Mirón, I., Criado, J., Linares, C., Díaz, J., 2013. Difficulties of defining the term, “heat wave”, in public health. *Int. J. Environ. Health Res.* 23, 377–379. <https://doi.org/10.1080/09603123.2012.733941>.
- Moss, R.H., Edmonds, J.A., Hibbard, K.A., Manning, M.R., Rose, S.K., van Vuuren, D.P., Carter, T.R., Emori, S., Kainuma, M., Kram, T., Meehl, G.A., Mitchell, J.F.B., Nakicenovic, N., Riahi, K., Smith, S.J., Stouffer, R.J., Thomson, A.M., Weyant, J.P., Wilbanks, T.J., 2010. The next generation of scenarios for climate change research and assessment. *Nature*. 463, 747–756. <https://doi.org/10.1038/nature08823>.
- Nairn, J., Fawcett, R., 2015. The excess heat factor: a metric for heatwave intensity and its use in classifying heatwave severity. *Int. J. Environ. Res. Public Health* 12, 227–253. <https://doi.org/10.3390/ijerph120100227>.
- Nairn, J., Ostendorf, B., Bi, P., 2018. Performance of excess heat factor severity as a global heatwave health impact index. *Int. J. Environ. Res. Public Health* 15, 2494. <https://doi.org/10.3390/ijerph15112494>.
- Pereira, S.C., Marta-Almeida, M., Carvalho, A.C., Rocha, A., 2017. Heat wave and cold spell changes in Iberia for a future climate scenario. *Int. J. Climatol.* 37, 5192–5205. <https://doi.org/10.1002/joc.5158>.
- Perkins, S.E., Alexander, L.V., 2013. On the measurement of heat waves. *J. Clim.* 26, 4500–4517. <https://doi.org/10.1175/JCLI-D-12-00383.1>.
- Perkins, S.E., Alexander, L.V., Nairn, J.R., 2012. Increasing frequency, intensity and duration of observed global heatwaves and warm spells. *Geophys. Res. Lett.* 39, L20714 <https://doi.org/10.1029/2012GL053361>.
- Raei, E., Nikoo, M.R., AghaKouchak, A., Mazdiyasni, O., Sadegh, M., 2018. GHWR, a multi-method global heatwave and warm-spell record and toolbox. *Sci. Data.* 5, 180206. <https://doi.org/10.1038/sdata.2018.206>.
- Ramos, A., Trigo, R., Santo, F., 2011. Evolution of extreme temperaturas over Portugal: recent changes and future scenarios. *Clim. Res.* 48, 177–192. <https://doi.org/10.3354/cr00934>.
- Randall, D.A., Wood, R.A., Bony, S., Colman, R., Fichefet, T., Fyfe, J., Kattsov, V., Pitman, A., Shukla, J., Srinivasan, J., Stouffer, R.J., Sumi, A., Taylor, K.E., 2007. Climate models and their evaluation. In: Solomon, S., Qin, D., Manning, M., Chen, Z., Marquis, M., Averyt, K.B., Tignor, M., Miller, H.L. (Eds.), *Climate Change 2007: The Physical Science Basis. Contribution of Working Group I to the Fourth Assessment Report of the Intergovernmental Panel on Climate Change*. Cambridge University Press, Cambridge, UK, and New York, NY, pp. 589–662.
- Rodríguez-Puebla, C., Encinas, A.H., García-Casado, L.A., y Nieto, S., 2010. Trends in warm days and cold nights over the Iberian Peninsula: relationships to large-scale variables. *Clim. Chang.* 100, 667–684. <https://doi.org/10.1007/s10584-009-9721-0>.
- Royé, D., Codesido, R., Tobías, A., Taracido, M., 2020. Heat wave intensity and daily mortality in four of the largest cities of Spain. *Environ. Res.* 182, 09027 <https://doi.org/10.1016/j.envres.2019.109027>.
- Russo, S., Dosio, A., Graversen, R.G., Sillmann, J., Carrao, H., Dunbar, M.B., Singleton, A., Montagna, P., Barbola, P., Vogt, J.V., 2014. Magnitude of extreme heat waves in present climate and their projection in a warming world. *J. Geophys. Res. Atmos.* 119, 12500–12512. <https://doi.org/10.1002/2014JD022098>.
- Russo, S., Sillmann, J., Fischer, E.M., 2015. Top ten European heatwaves since 1950 and their occurrence in the coming decades. *Environ. Res. Lett.* 10 (12), 124003. <https://doi.org/10.1088/1748-9326/10/12/124003>.
- Sánchez-Benítez, A., Barriopedro, D., García-Herrera, R., 2020. Tracking Iberian heatwaves from a new perspective. *Weather Clim. Extrem.* 28, 100238. <https://doi.org/10.1016/j.wace.2019.100238>.
- Scalley, B., Spicer, T., Jian, L., Xiao, J., Nairn, J., Robertson, A., Weeramanthri, T., 2015. Responding to heatwave intensity: excess Heat factor is a superior predictor of health service utilisation and a trigger for heatwave plans. *Aust. N. Z. J. Public Health* 39, 582–587. <https://doi.org/10.1111/1753-6405.12421>.
- Schleussner, C., Pfleiderer, P., Fischer, E., 2017. In the observational record half a degree matters. *Nat. Clim. Chang.* 7, 460–462. <https://doi.org/10.1038/nclimate3320>.
- Schoetter, R., Cattiaux, J., Douville, H., 2015. Changes of western European heat wave characteristics projected by the CMIP5 ensemble. *Clim. Dyn.* 45, 1601–1616. <https://doi.org/10.1007/s00382-014-2434-8>.
- Son, J., Bell, M., Lee, J., 2014. The impact of heat, cold, and heat waves on hospital admissions in eight cities in Korea. *Int. J. Biometeorol.* 58, 1893–1903. <https://doi.org/10.1007/s00484-014-0791-y>.
- Taylor, K.E., Stouffer, R.J., Meehl, G.A., 2012. An overview of Cmp5 and the experiment design. *Bull. Am. Meteorol. Soc.* 93, 485–498. <https://doi.org/10.1175/BAMS-D-11-0094.1>.
- Tullet, I., 2000. *Climatología de España y Portugal*, 76. Editorial, Universidad de Salamanca, Spain.
- Vicedo-Cabrera, A.M., Guo, Y., Sera, F., et al., 2018. Temperature-related mortality impacts under and beyond Paris Agreement climate change scenarios. *Clim. Chang.* 150, 391. <https://doi.org/10.1007/s10584-018-2274-3>.
- Vicente, C., Pereira, S.C., y Rocha, A., 2019. Climate change projections of extreme temperatures for the Iberian Peninsula. *Atmosphere*. 10, 229. <https://doi.org/10.3390/atmos10050229>.
- Wilcoxon, F., 1945. Individual comparisons by ranking methods. *Biometrics*. 1, 80–83.
- Williams, S., Venugopal, K., Nitschke, M., Nairn, J., Fawcett, R., Beattie, C., Wynwood, G., Bi, P., 2018. Regional morbidity and mortality during heatwaves in South Australia. *Int. J. Biometeorol.* 62, 1911. <https://doi.org/10.1007/s00484-018-1593-4>.
- Wolf, T., McGregor, G., 2013. The development of a heat wave vulnerability index for London, United Kingdom. *Weather Clim. Extrem.* 1, 59–68. <https://doi.org/10.1016/j.wace.2013.07.004>.
- Wu, C.H., Yeh, P.J.-F., Ju, J.L., Chen, Y.Y., Xu, K., Dai, H., Niu, J., Hu, B.X., Huang, G.R., 2021. Assessing the spatio-temporal uncertainties in future meteorological droughts from CMIP5 models, emission scenarios and bias corrections. *J. Clim.* 34 (5), 1903–1922. <https://doi.org/10.1175/JCLI-D-20-0411.1>.
- Xu, Z., Fitz Gerald, G., Guo, Y., Jalaludin, B., Tong, S., 2016. Impact of heatwave on mortality under different heatwave definitions: a systematic review and meta-analysis. *Environ. Int.* 89–90, 193–203. <https://doi.org/10.1016/j.enenvint.2016.02.007>.
- Zander, K., Botzen, W., Oppermann, E., Kjellstrom, T., Garnett, S.T., 2015. Heat stress causes substantial labour productivity loss in Australia. *Nat. Clim. Chang.* 5, 647–651. <https://doi.org/10.1038/nclimate2623>.